

Study of Integrated Rural Electrification System Using Wind-Biogas Based Hybrid System and Limited Grid Supply System

D. K. Yadav^{*†}, T. S. Bhatti^{*} and Ashu Verma^{*}

^{*} Centre for Energy Studies, IIT Delhi

Hauz Khas, New Delhi, PIN: 110016, India

(dky_b@yahoo.com, tsbhatti@yahoo.com, averma@ces.iitd.ac.in)

[†] Corresponding Author; Research Scholar, CES IIT Delhi,

Tel: +91 9414453513, dky_b@yahoo.com

Received: 19.06.2016 Accepted: 12.09.2016

Abstract- This paper presents modeling of system having wind-biogas based hybrid system operating in parallel with limited grid supply system to meet the rural demand, of a cluster of villages continuously. In this integrated rural electrification system (IRES), a fixed part of the power is supplied by the grid and the remaining power, required by the load under steady state and also the variations, is taken care by a hybrid renewable energy system (HRES). The wind energy converting system (WECS) uses a permanent magnet synchronous generator (PMSG) and synchronized in the hybrid system through a voltage source converter (VSC). The other source considered in the hybrid system is biogas-genset equipped with electronic speed governor and synchronous generator (SG) with automatic voltage regulator (AVR).

The variation in load and/or input wind power to WECS may cause deviation in frequency and voltage and to maintain these parameters at nominal values, the power generated by biogas-genset is controlled, through governor control. The basic control schemes for frequency and magnitude of system voltage may not ensure limited grid operation. Therefore the system model is unique as it considers the dynamics and control of system voltage angle also. The main contribution of this paper is the system dynamic model development and its performance study. Proportional integral (PI) controllers are used in the model and their values are optimized using integral square error (ISE) criteria. Finally, the system simulation results have been shown for step deviations in load and/or input wind power to the WECS.

Keywords- Integrated rural electrification system, WECS, PMSG, biogas-genset, hybrid renewable energy system, limited grid supply system.

1. Introduction

Globally more than 1.2 billion people are deprived of proper electricity access especially in rural areas [1, 2, 4]. In India major population is living in rural areas with no electricity or electricity available with load shedding occurring for hours or it may be number of intermittent load shedding per day. Continuous availability of electric supply can be key driver in rural development to uplift their living standards [3]. With the present infrastructure and growth rate of conventional generation, it is not possible to meet the load demand even of urban and industrial sectors in India. The gap between electric supply and demand is widening every year. On the other hand there is tremendous potential of

renewable energy sources (RES) in rural areas. The possible options of RES that may be available at a site are biomass/biogas, wind, small hydro, solar PV etc. The grid, a feeder of a distribution substation, is supplying a certain amount of energy E , to a cluster of villages/towns by scheduling of load shedding over a day. It is considered that the same amount of energy will be drawn from the grid over a day but there will be no load shedding so that $E =$ reduced power (but constant) $\times 24$ hrs. It has been introduced as limited grid supply system. It means in spite of taking full load power for few hours from grid, a partial but fixed power (limited power) can be supplied by the grid utility continuously for 24 hours and the remaining power can be obtained from a combination of renewable sources to feed

the system load. The operation of HRES is in parallel with grid but not in isolation.

The use of RES is requirement of time due to environmental concern and limited stock of conventional fuels for power generation [5]. The biogas based electric generation will be sufficient to meet the local electric demand as the biomass available from forest and crops in rural India is considerable [6]. Advancement in technology has made it reliable and controllable source of electric power in comparison to WECS [6, 7]. Due to the local availability of the source, biogas-gensets can be used in place of diesel-gensets in HRESs. The biogas-gensets commonly uses SG having exciter control with AVR [8, 9] and in some applications uses induction generator [10]. Numbers of studies have been carried out on biogas and wind based HRES [11, 12] and biogas and PV based HRES [13-15]. The development of WECS is fast as compared to other renewable energy options [16]. Initially induction generators were used in WECS [17] having advantage of no synchronization but they have poor voltage regulation.

Doubly fed induction generators (DFIG) and PMSG are now commonly used to efficiently tap power under variable speed operation of WECS [16, 18-22]. The PMSG based variable speed WECS, uses VSC as frequency converter for interconnection to the outer network [19, 20] and it has active and reactive power control capability [21, 22]. Though PMSG is costly but it has high efficiency, low maintenance, operation at low speeds with no gears etc. [22, 23]. In RES based hybrid power systems it is very difficult to control voltage and frequency due to intermittent nature of the sources. Number of control schemes for frequency and/or voltage for isolated hybrid power systems are available [23-28]. Advanced energy management schemes developed with dynamic control for a stand-alone hybrid energy system [29]. Different energy control schemes for RES based HPS are given in [30] for its efficient operation. The power flow of the grid tied inverter is controlled using PSO in a RES based HPS [31]. Some techniques use energy storage for frequency control, and SVC or load side converter for reactive power control. In small hybrid systems the fluctuations in frequency and voltage occurs with load deviations and/or deviation in renewable sources of power and as the renewable sources are intermittent in nature decoupled control may not be possible, therefore simultaneous control of both parameters is necessary.

In the proposed scheme of IRES the load demand is supplied by a wind-biogas hybrid system with limited grid. For dynamic stability studies the IRES is modelled for simultaneous control of system voltage (magnitude and angle), and frequency. The biogas-genset includes biogas engine model with electronic speed governor [9] and SG with AVR and IEEE type-I exciter model [26]. The mathematical modelling and control techniques of PMSG based WECS for reactive power control as given in [17, 18, 32] are used and the same is extended for real power also. The modelling is typical as it also includes the deviation in system voltage angle as state variable. The PI controllers used are tuned using ISE criteria to enhance the dynamic performance of the system.

2. Integrated Rural Electrification System Modeling

An integrated rural electrification system consisting of wind-biogas based hybrid system and limited grid supply system is considered for mathematical modeling. The single line diagram of the system considered is shown in "Fig.1". The system power balance equations are given by

$$P_B + P_W + P_G = P_L \quad (1)$$

$$Q_B + Q_W + Q_G = Q_L \quad (2)$$

For small perturbation the power balance equations. (1) and (2) can be written as

$$\Delta P_B + \Delta P_W + \Delta P_G = \Delta P_L \quad (3)$$

$$\Delta Q_B + \Delta Q_W + \Delta Q_G = \Delta Q_L \quad (4)$$

The difference in the deviation of real power generation and the deviation of real power load will result in the system frequency deviation which can be expressed in state space eqn. using Laplace transform as

$$\Delta F(s) = \frac{K_P}{1+sT_P} [\Delta P_B(s) + \Delta P_W(s) + \Delta P_G(s) - \Delta P_L(s)] \quad (5)$$

The difference in the deviation of reactive power generation and deviation of reactive power load will cause the system bus voltage deviation which can be expressed in state space eqn. using Laplace transform [17, 32] as

$$\Delta V(s) = \frac{K_V}{1+sT_V} [\Delta Q_B(s) + \Delta Q_W(s) + \Delta Q_G(s) - \Delta Q_L(s)] \quad (6)$$

The modeling of the different components of the system shown in "Fig. 1" are given in subsequent sections.

2.1. Modeling of WECS

The WECS comprises wind turbine (WT) coupled with PMSG and produces power having variable frequency and voltage depending upon wind speed and turbine characteristics. The machine side AC- DC converter transfer the active power of the PMSG to the load side DC- AC converter through a coupling capacitor between converters by maintaining constant voltage across it. The DC-AC converter is VSC matches the voltage and frequency of the generated power with the values of the system bus voltage and frequency. In addition the VSC also maintains the system reactive power balance, therefore no additional reactive power compensation device is required for the system.

A small signal model of the WECS is developed using active and reactive power output equations [17, 32] given by

$$P_W = \frac{V_{inW} V \sin(\delta_{inW} + \theta)}{X_{TW}} \quad (7)$$

$$Q_W = \frac{V_{inW} V \cos(\delta_{inW} + \theta) - V^2}{X_{TW}} \quad (8)$$

For small incremental change in the active and reactive power outputs of the WECS, equations (7) and (8) can be written as

$$\Delta P_w(s) = K_{w1}\Delta\delta_{inw}(s) + K_{w2}\Delta\theta(s) + K_{w3}\Delta V_{inw}(s) + K_{w4}\Delta V(s) \quad (9)$$

and

$$\Delta Q_w(s) = K_{w5}\Delta\delta_{inw}(s) + K_{w6}\Delta\theta(s) + K_{w7}\Delta V_{inw}(s) + K_{w8}\Delta V(s) \quad (10)$$

The parameters/constants V_{inw} , δ_{inw} , K_{w1} , K_{w2} , --- K_{w8} , associated with state variables are given in the "Appendix-I".

The transfer function block diagram of the WECS under consideration with real and reactive power control is shown in "Fig. 2". The function of the proportional integral controllers PI1 and PI2 is to set $\Delta\delta_{inw}$ and ΔV_{inw} of the inverter such that $\Delta P_w = \Delta P_{Iw}$ under steady state conditions. Also the reactive power ΔQ_w generated under steady state

condition aids with the other system reactive power in elimination of the variation in system voltage, ΔV .

2.2. Modeling of Biogas-Genset

The transfer function block diagram of biogas-genset having electronic speed governor system [9] is shown in "Fig. 3". The biogas is supplied to the engine through a valve and the valve position is adjusted by the actuator depending upon the signal generated by the electronic speed governor in response to system frequency and voltage angle change. The change in active power output of the biogas-genset is given by

$$\Delta P_B(s) = \frac{1}{1 + sT_{B7}} \Delta X_{VB}(s) \quad (11)$$

The change in the input valve position, $\Delta X_{VB}(s)$ set by the actuator is given by

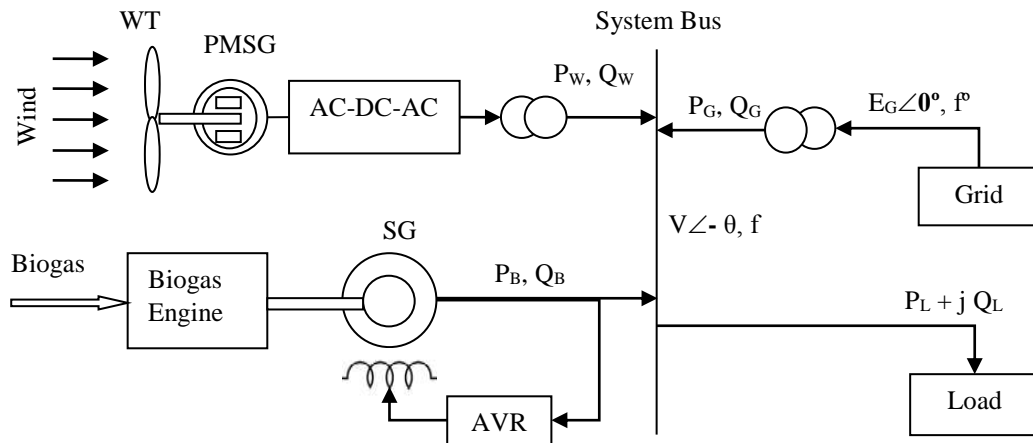


Fig.1 IRES using wind & biogas based hybrid system and limited grid supply.

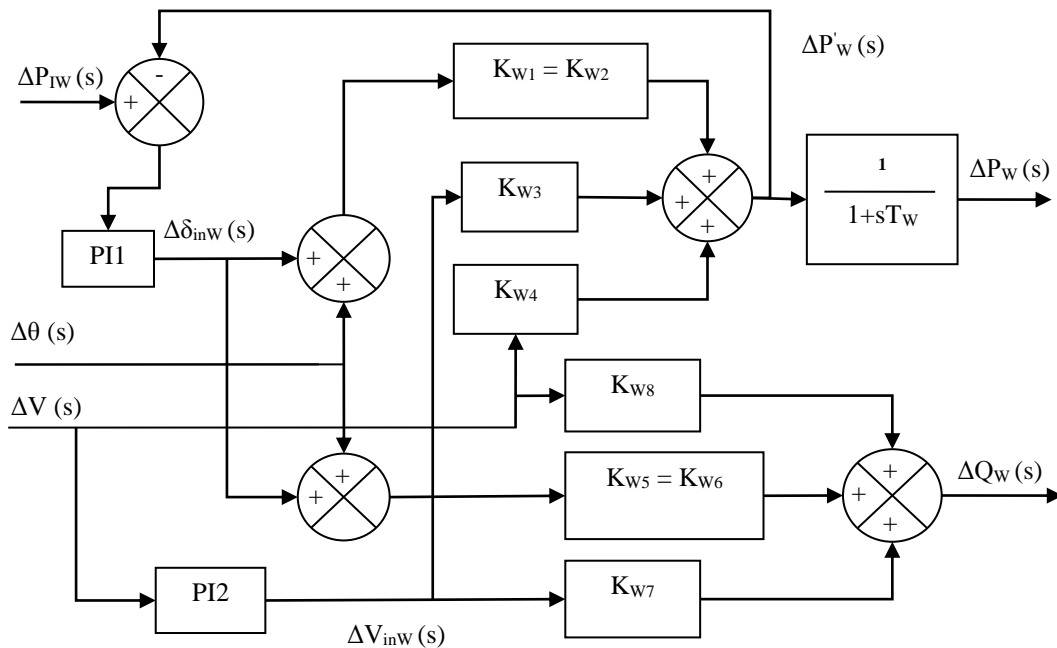


Fig. 2: Transfer function model of WECS with PMSG and converter.

$$\Delta X_{VB}(s) = \frac{(1 + sT_{B4})}{s(1 + sT_{B5})(1 + sT_{B6})} \Delta X_{AB}(s) \quad (12)$$

The change in the actuator input depends upon the electronic speed governor design and it is given by

$$\Delta X_{AB}(s) = \frac{(1 + sT_{B3})}{(1 + sT_{B1} + s^2T_{B1}T_{B2})} \Delta P_{CB}(s) \quad (13)$$

The biogas-genset is considered to have an IEEE type-I excitation control system with saturation neglected as shown in “Fig. 4” [17, 32]. The small deviation in voltage behind transient reactance, $\Delta E'_{qB}(s)$ [17, 25, 26, 32], is given by

$$(1 + sT_{GB})\Delta E'_{qB}(s) = [K_{1B}\Delta E_{f1B}(s) + K_{2B}\Delta V(s)] \quad (14)$$

For small deviation in system voltage, the reactive power injected by the biogas-genset is given by

$$\Delta Q_B(s) = K_{3B}\Delta E'_{qB}(s) + K_{4B}\Delta V(s) \quad (15)$$

Assuming that SG is operating at constant power factor, the reactive power change due to change in real power is given by

$$\Delta Q'_B(s) = K_{RB}\Delta P_B(s) \quad (16)$$

The parameters/constants T_{GB} , K_{1B} , K_{2B} , K_{3B} , K_{4B} , and K_{RB} are given in “Appendix-I”.

2.3. Grid Model

In a grid connected system, the transformer is used to adjust the secondary winding voltage level and make it equal to the system bus voltage. The voltage on the transformer primary side is considered to be constant. The representation of a short feeder line, resistance neglected, including transformer is shown in “Fig. 5”.

The small change in real and reactive power of the grid can be written in state variables

$$\Delta P_G(s) = K_{1G}\Delta\theta(s) + K_{2G}\Delta V(s) \quad (17)$$

$$\Delta Q_G(s) = K_{3G}\Delta\theta(s) + K_{4G}\Delta V(s) \quad (18)$$

The constants K_{1G} , K_{2G} , K_{3G} , and K_{4G} are given in “Appendix-I”.

The change in system bus voltage angle with change in system frequency is given by

$$\Delta\theta(s) = \frac{2\pi}{s} \Delta F(s) \quad (19)$$

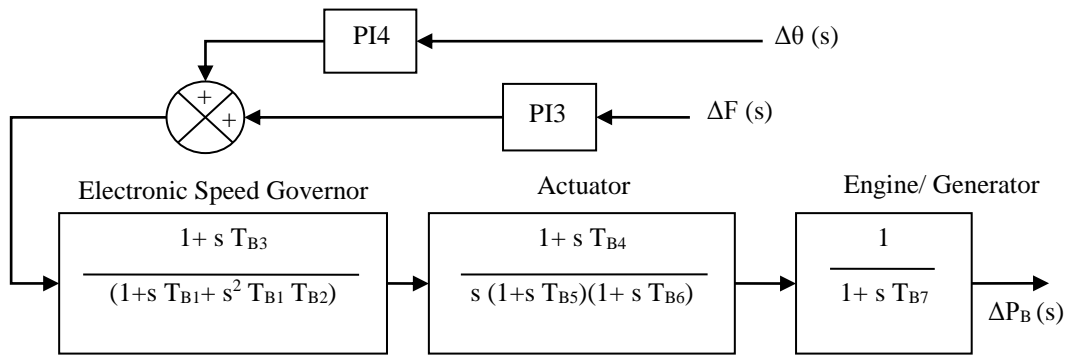


Fig. 3: Transfer function model of biogas-genset for real power control.

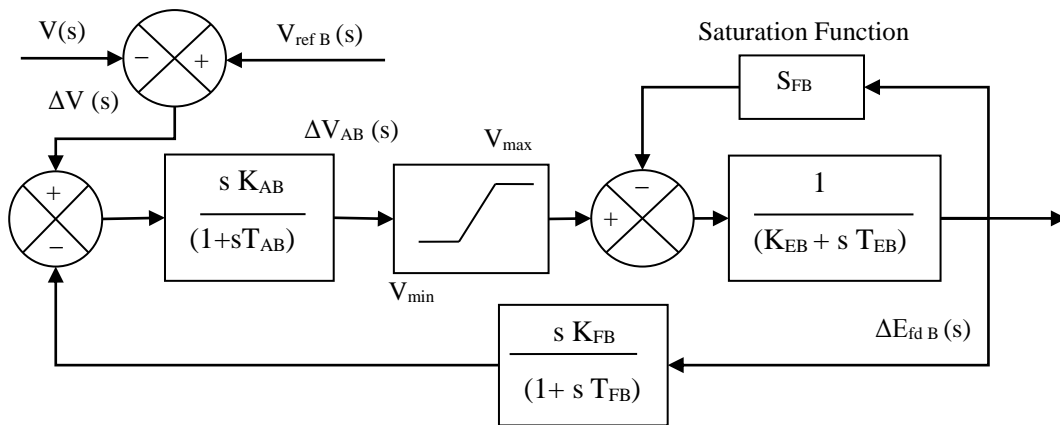


Fig. 4: Model of IEEE Type-I excitation control system (with saturation neglected) for biogas-genset.

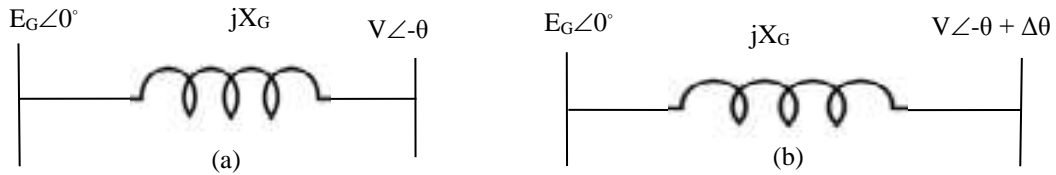


Fig. 5: Model of short feeder line per phase (a) before disturbance and (b) after disturbance.

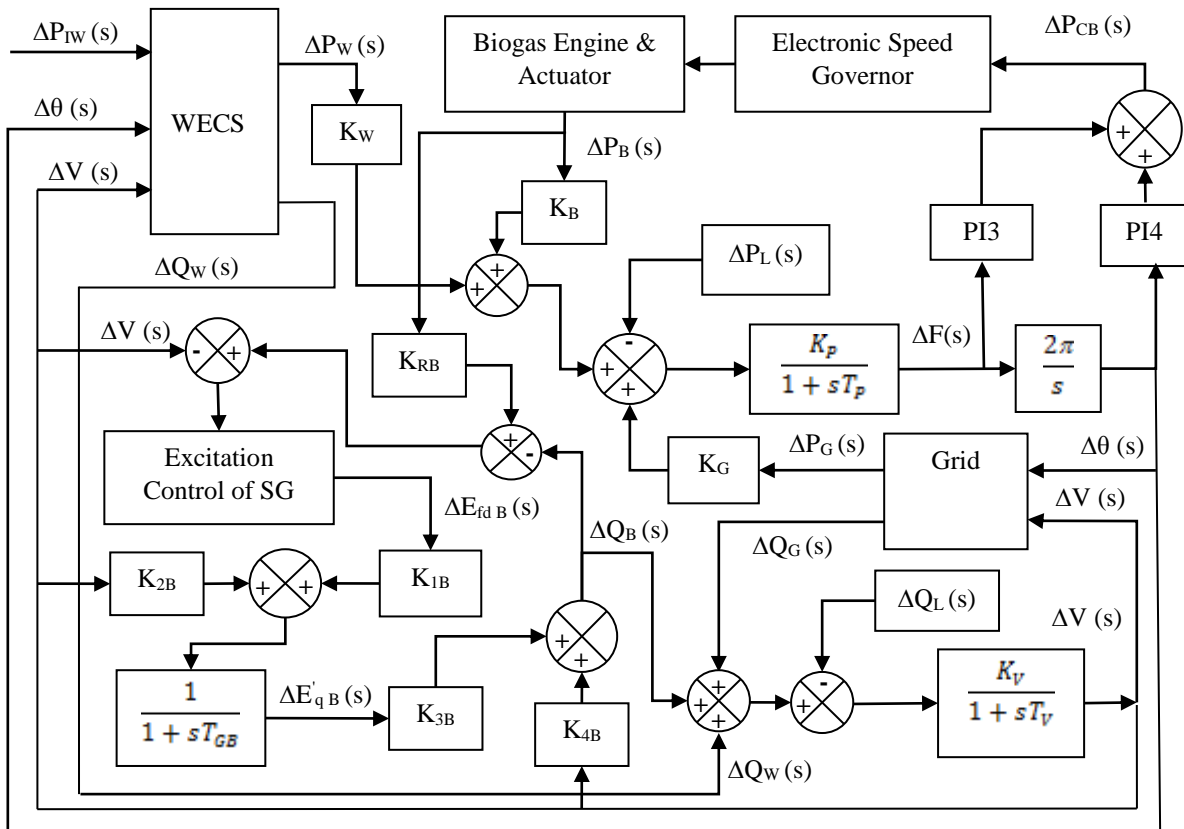


Fig. 6 Transfer function model of the Integrated Rural Electrification System.

3. System Simulation and Results

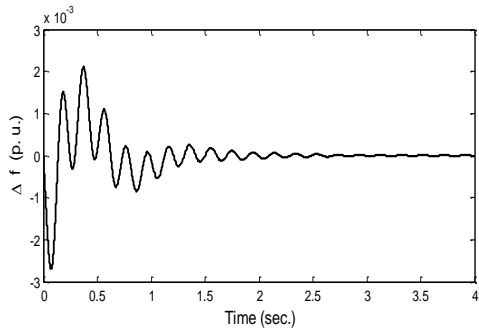
The transfer function model of the integrated rural electrification system using wind-biogas based hybrid system and limited grid supply system is shown in “Fig. 6”. All the three sources are contributing to meet a load demand of 1MW and the data used for simulation of the system is given in “Appendix-II”. The power supplied by the grid is 300 kW with 30% participation factor and 70% is supplied by the renewable sources given in “Table T1 in Appendix-II”. The dynamic results of simulation are obtained when system is subjected to step change in load with or without step change in wind power input. The gains of the PI controllers of Figs. 2 & 3 are optimized using ISE criterion and the values are given in “Table 1”.

A system disturbance comprising step increase of 1% in active and reactive power load without change in wind power input has been considered and the transient responses are shown in “Fig. 7”. It has been observed that the oscillations in Δf and Δθ settles within 3 sec. with zero steady state error

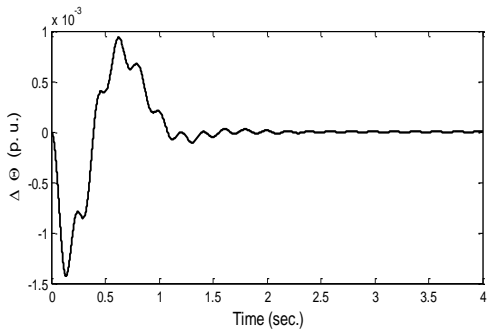
as shown in “Fig. 7 (a) and (b)”, respectively. The real power change in ΔP_L = 0.01 pu has been provided by the biogas genset under steady state conditions as shown in “Fig. 7(c)”. There is no change in input wind power, therefore ΔP_w = 0 under steady state conditions as shown in “Fig. 7(d)”. Our strategy is not to draw any additional power from grid under steady state conditions, which is true as ΔP_G = 0, as shown in “Fig. 7(e)”. The reactive power demand ΔQ_L = 0.01 pu has been met by biogas genset and the WECS VSC under steady state conditions, therefore the deviations in system voltage, ΔV and grid reactive power, ΔQ_G are zero as shown in “Fig. 7(f) - (j)”. The control of voltage is fast but the reactive power control is slow as it has the effect of real power dynamics. None of the studies have accounted for the change in reactive power with change in real power of synchronous generators. In this study it has been incorporated that as the real power increases the reactive power also increases as shown in Fig. “7(c) and (g)” and WECS VSC supplies the reactive power initially.

Table 1: Values of PI controller gain parameters.

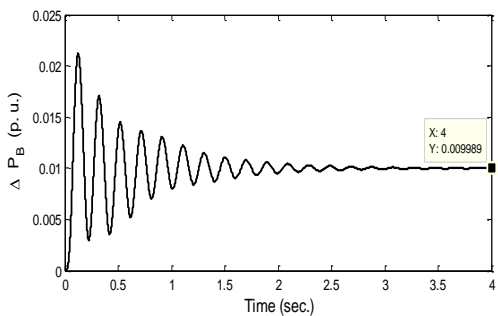
Controller	Gain	ISE tuned gain values
PI 1	K_{P1}	-0.244
	K_{I1}	1686.10
PI 2	K_{P2}	-6.04
	K_{I2}	-44626.00
PI 3	K_{P3}	-42.00
	K_{I3}	-91.50
PI 4	K_{P4}	-20.00
	K_{I4}	-212.50



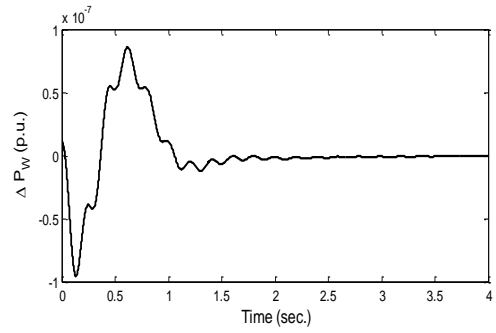
(a) Change in system frequency, Δf .



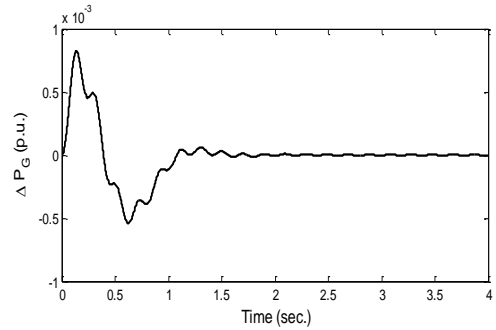
(b) Change in system voltage angle, $\Delta\theta$.



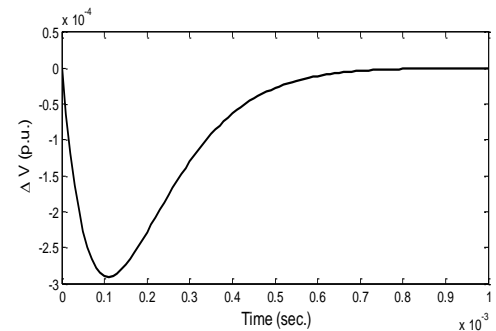
(c) Change in active power of biogas genset, ΔP_B .



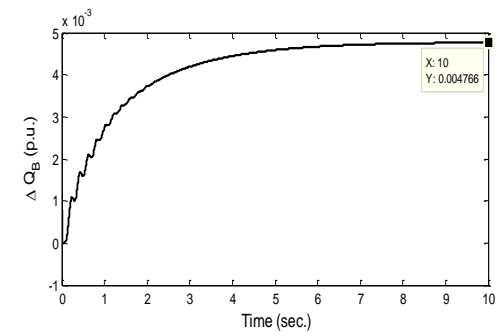
(d) Change in active power of WECS, ΔP_W .



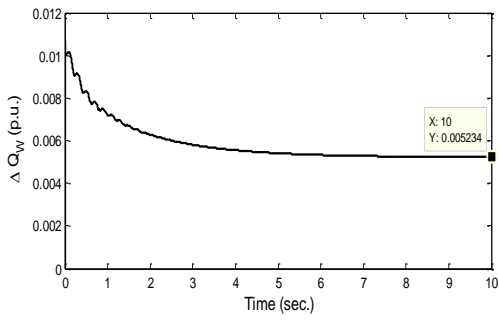
(e) Change in active power supply of grid, ΔP_G .



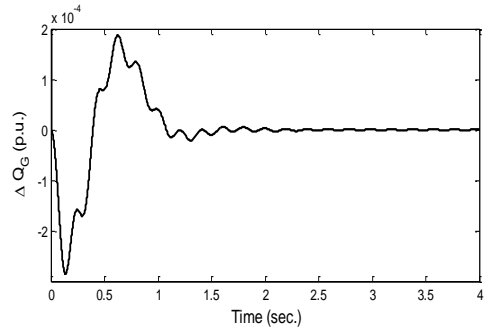
(f) Change in system voltage, ΔV .



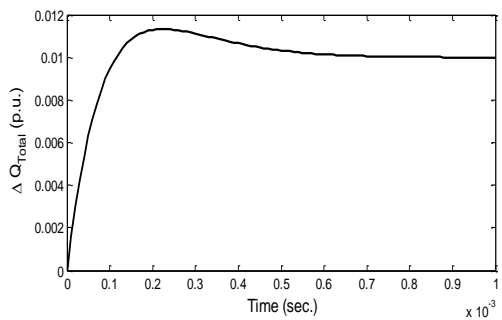
(g) Change in reactive power of biogas genset, ΔQ_B .



(h) Change in reactive power of WECS, ΔQ_w .



(i) Change in reactive power supply of grid, ΔQ_G .



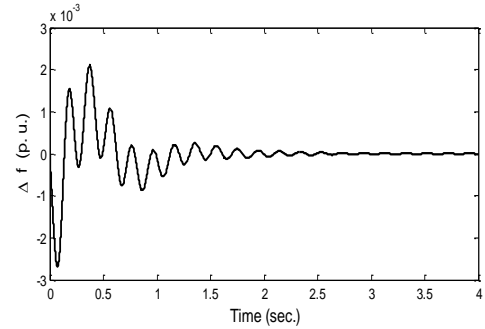
(j) Change in total reactive power of IRES.

Fig. 7 Dynamic responses of IRES for 1% step increase in real and reactive power of load without change in wind input power.

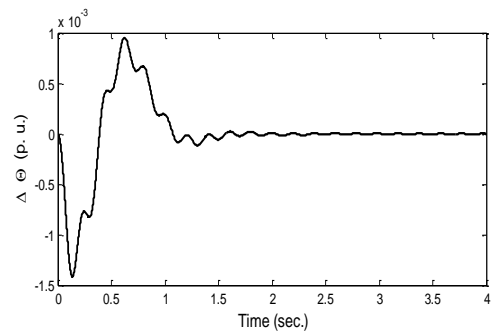
A step increase of 1% in active and reactive power load with 1% step increase in wind power input have been considered as system disturbances and the transient responses are shown in “Fig. 8”. It has been observed that the dynamic responses of deviation in system frequency and system voltage angle settles within 3 sec. with zero steady state error as shown in “Fig. 8 (a) and (b)”, respectively. The real power change in $\Delta P_L = 0.01$ pu has been provided partly by increase in power generation of WECS, $\Delta P_w = 0.01 \times K_w = 0.00133$ pu and remaining by the biogas genset $\Delta P_B = 0.00867$ pu under steady state conditions as shown in “Fig. 8 (c) and (d)”, respectively. The control strategy is not to draw any additional power from grid under steady state conditions, which is true as $\Delta P_G = 0$, as shown in “Fig. 8 (e)”.

Though the fluctuations get eliminated in about 3 sec. but the steady state error takes longer time to vanish due to inertia of the wind turbine. The reactive power demand, $\Delta Q_L = 0.01$ pu has been met by biogas genset and the VSC of WECS under steady state conditions as shown in “Fig. 8 (g)

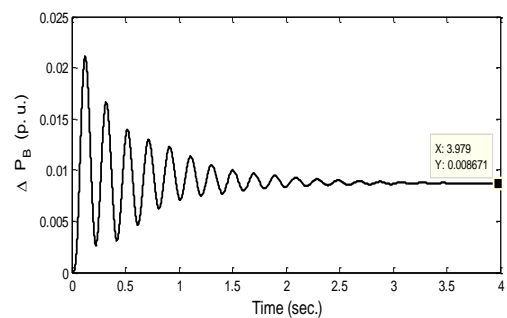
and (h)”. Therefore the deviations in system voltage, ΔV and grid reactive power, ΔQ_G are zero as shown in “Fig. 8 (f) and (i)”. The WECS VSC eliminates the system voltage deviations in 0.001 sec. But the overall reactive power control is slow due to the involvement of real power dynamics. Again in case of biogas genset as the real power increases the reactive power also increases as shown in “Fig. 8 (d) and (g)” and WECS VSC compensates full reactive power initially.



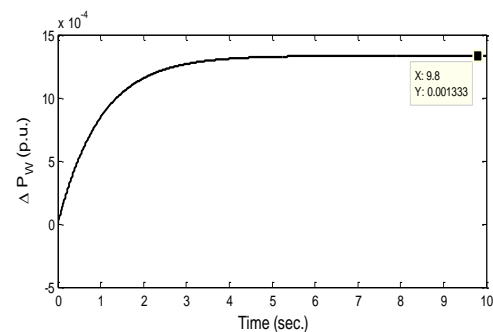
(a) Change in system frequency, Δf .



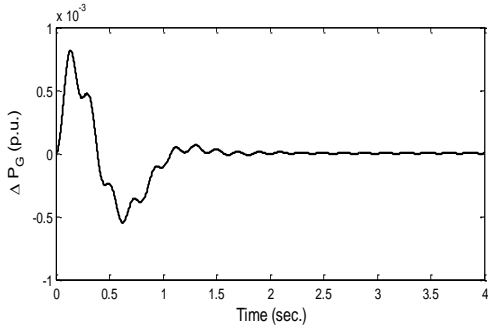
(b) Change in system voltage angle, $\Delta \theta$.



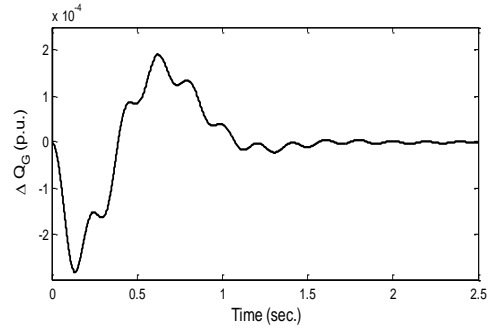
(c) Change in active power of biogas genset, ΔP_B



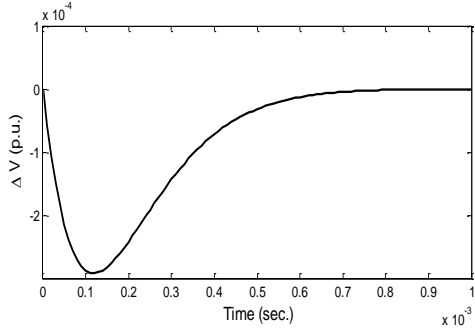
(d) Change in active power of WECS, ΔP_w



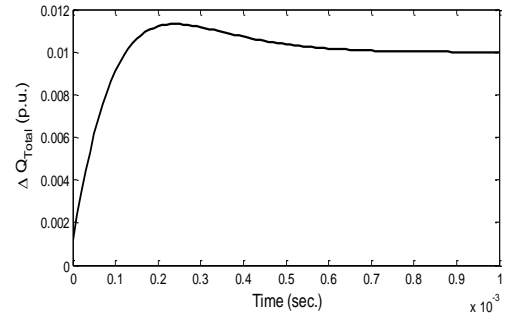
(e) Change in active power supply of grid, ΔP_G .



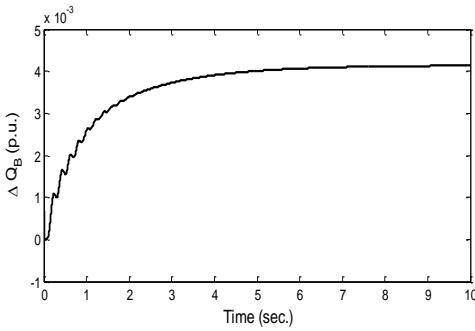
(i) Change in reactive power supply of grid, ΔQ_G .



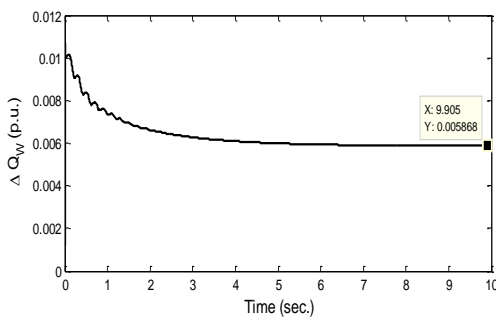
(f) Change in system voltage, ΔV .



(j) Change in total reactive power of IRES.



(g) Change in reactive power of biogas genset, ΔQ_B .



(h) Change in reactive power of WECS, ΔQ_W .

Fig. 8 Deviations of state variables when load and wind input power both are changing.

4. Conclusion

A scheme of integrated rural electrification system with limited grid supply system has been proposed. In the proposed scheme of IRES the load demand has been supplied by a wind-biogas hybrid system along with limited grid. The operation of hybrid renewable energy system has been considered in parallel with grid but not in isolation. Also in small hybrid system the fluctuations in frequency and voltage occurs with load deviations and/or deviation in renewable sources of power and as the renewable sources are intermittent in nature decoupled control may not be possible, therefore simultaneous control of frequency, voltage and reactive power is necessary. For dynamic stability studies the mathematical modeling of system has been presented which is typical as it also includes the deviation in system voltage angle as state variable to maintain limited grid operation. Therefore the main contribution of the paper is the development of transfer function model of such a system for dynamic performance study. PI controllers have been used in the model to enhance the dynamic performance of the system and their values have been optimized using integral square error (ISE) criteria.

The system simulation results have been shown for step deviations in real and reactive power load with and without change in wind power input. From the transient responses it has been observed that the mismatch in real power load is eliminated by corresponding change in real power generation from biogas genset under steady state conditions. Similarly if there is change in wind power input and mismatch in real power load, then the corresponding real power generation from biogas genset will balance the offset. It has been

observed that in no way it will affect the grid power generation under steady state conditions, and which is the main objective of this study. The synchronous generator operates at a typical power factor and the reactive power generation is a function of real power generated, though AVR regulates its terminal voltage by excitation control. The effect of change in reactive power due to change in real power of biogas genset has been taken into account in the transfer function model of the system. It has been observed that the system voltage deviations gets eliminated in 0.001 secs. with $\Delta V = 0.0$ under steady state conditions, but the overall reactive power control is slow due to the involvement of real power dynamics. The control strategy was not to draw any additional power from grid which is also true as grid reactive power, ΔQ_G is zero under steady state conditions.

References

- [1] International Energy Agency (IEA) annual report 2013 (www.iea.org).
- [2] M. Millinger, T. Mårilind, and E.O. Ahlgren, "Evaluation of Indian rural solar electrification: A case study in Chhattisgarh", *Energy for Sustainable Development*, 16 (2012), pp. 486–492.
- [3] James Cust, Anoop Singh and Karsten Neuhoff, "Rural electrification in India: Economic and industrial aspects of renewables", (2007), pp. 1-36.
- [4] C. L. Azimoh, P. Klintonberg, F. Wallin, B. Karlsson, C. Mbohwa, "Electricity for development: Mini-grid solution for rural electrification in South Africa", *International Journal of Energy Conversion and Management* 110 (2016) 268–277.
- [5] E. N. Azadani, S. Member, C. Canizares, and K. Bhattacharya, "Modeling and stability analysis of distributed generation," 2012 *IEEE Power and Energy Society General Meeting*, pp. 1–8.
- [6] P. Balamurugan, S. Kumaravel, and S. Ashok, "Optimal operation of biomass gassifier based hybrid energy system," *ISRN Renew. Energy*, Sept. 26, 2011, pp. 1–7.
- [7] Z. Yanning, K. Longyun, C. Binggang, H. Chung-Neng, and W. Guohong, "Renewable energy distributed power system with wind power and biogas generator," 2009 *IEEE Transmission & Distribution Conference & Exposition: Asia and Pacific*, vol. 4, Oct 26, 2009, pp. 1–6.
- [8] H. Tehzib, M. Z. Rashid, J. M. Keerio, and B. Asad, "Simulation of combined photovoltaic, Thermal & biogas hybrid system," *International Journal of Electrical & Computer Science, IJECS-IJENS*, Vol. 12, No. 05, 2012, pp. 83-89 .
- [9] L. Wang, and P. Lin, "Analysis of a commercial biogas generation system using a gas engine – induction generator set," *IEEE Transactions on Energy Conversion*, Vol. 24, No. 1, March 2009, pp. 230–239.
- [10] A. Perez-Navarro, D. Alfanzo, C. Alvarez, F. Ibanez, C. Sanchez and I. Segura, "Hybrid biomass-wind power plant for reliable energy generation", *Renewable Energy* 35 (2010), pp. 1436-1443.
- [11] Francisco Jurado, Jose R. Saenz, "Possibilities for biomass-based power plant and wind system integration", *Energy* 27(2002), pp. 955-966.
- [12] M. R. Borges Neto, P.C.M. Carvalho, J.O.B. Carioca and F.J.F. Canafistula, "Biogas/photovoltaic hybrid power system for decentralized energy supply of rural areas", *Energy Policy* 38(2010), pp. 4497-4506.
- [13] J. Servert, G. San Miguel and D. Lopez, "Hybrid solar-biomass plants for power generation; Technical and economic assessment", *Global NEST Journal*, Vol. 13, No. 3, 2011, pp. 266-276.
- [14] Xu Zhenjun, "Model and performance for direct supplying energy system by biogas", *IEEE International Conference on New Technology of Agricultural Engineering (ICAE)*, 2011, pp. 751-754.
- [15] V. Jerković, "Stability testing of a small biogas plant in an electric power system," *International Journal of Electrical and Computer Engineering Systems*, Volume 2, Number 2, 2011, pp. 49–54.
- [16] Suhui Li, Haskew, Tim A., Eduard Muljadi and Cristina Serrentino, "Characteristic study of vector controlled direct drive permanent magnet synchronous generator in wind power generation", *Electric Power Components and Systems*, Volume 37, Issue 10, 2009, pp. 1162-1179.
- [17] R. C. Bansal, "Modelling and automatic reactive power control of isolated wind-diesel hybrid power systems using ANN", *International Journal of Energy Conversion and Management* 49 (2008), pp. 357–364.
- [18] Sasi C. and G. Mohan, "Comparative analysis of an integration of a wind energy conversion system of PMSG and DFIG models connected to power grid", *International Journal of Electrical Engineering*, Volume 6, Number 3 (2013), pp. 231-248.
- [19] M. K. Deshmukh and S. S. Deshmukh, "Modeling of hybrid renewable energy systems," *Renew. Sustain. Energy Rev.*, vol. 12, no. 1, Jan. 2008, pp. 235–249.
- [20] Hui Zheng, Yu Zhu and Liu Jinsong, "Verification of DFIG and PMSG wind turbines' LVRT characteristics through field testing", *IEEE International Conference on Power System Technology (POWERCON)*, 2012, pp. 1-6.

[21] H. Li, and Z. Chen, "Overview of different wind generator systems and their comparisons", *IET Renewable Power Generation*, 2008, pp. 123-138.

[22] Wu, Bin, Lang, Y., Zargari, N. and Kouro, S., "Power conversion and control of wind energy systems" *IEEE Press, John Wiley & Sons, Inc.*, Hoboken, New Jersey, 2011, pp. 1-453.

[23] Prakash K. Roy, Vijay P. Singh, Soumya R. Mohanty, Nand Kishor and Sumit Sen," Frequency control based on H_∞ controller for small hybrid power system", *The 5th International Power Engineering and Optimization Conference (PEOCO2011)*, Shah Alam, Selangor, Malaysia : 6-7 June 2011, pp. 227-232.

[24] Shailendra Singh, Sameer Kumar Singh, Saurabh Chanana and Y. P. Singh," Frequency regulation of an isolated hybrid power system with battery energy storage system", *IEEE Power and Energy Systems: Towards Sustainable Energy (PESTSE 2014)*, Mar 13, 2014, pp. 1-6.

[25] R. C. Bansal, "Automatic reactive-power control of isolated wind-diesel hybrid power Systems", *IEEE Transactions on Industrial Electronics*, Vol. 53, No. 4, August 2006, pp. 1116-1126.

[26] D. K. Yadav and T. S. Bhatti, "Voltage control through reactive power support for WECS based hybrid power system", *International Journal of Electrical Power & Energy Systems, Volume 62, November 2014*, pp. 507-518.

[27] Yang, Shun and Zhang, Lida, "Modeling and control of the PMSG wind generation system with a novel controller", *Third International Conference on Intelligent System Design and Engineering Applications*, 2013, pp. 946-949.

[28] Lara O. A., Jenkins N., Ekanayake, J., Cartwright P. and Hughes M., "Wind energy generation modeling and control", *John Wiley & Sons, Ltd 2009*, ISBN: 978-0-470-71433-1, pp 1-269.

[29] Tareq Alnejaili, Said Drid, Driss Mehdi, et. al., "Dynamic control and advanced load management of a stand-alone hybrid renewable power system for remote housing", *International Journal of Energy Conversion and Management* 105 (2015), pp. 377-392.

[30] Nicu Bizon, Mihai Oproescu, Mircea Raceanu "Efficient energy control strategies for a Standalone Renewable/Fuel Cell Hybrid Power Source", *International Journal of Energy Conversion and Management* 90 (2015), pp. 93-110.

[31] Pablo García-Triviño, Antonio José Gil-Mena, Francisco Llorens-Iborra, et. al., "Power control based on particle swarm optimization of grid-connected inverter for hybrid renewable energy system",

International Journal of Energy Conversion and Management 91 (2015), pp. 83-92.

[32] Sharma Pawan, "Automatic Reactive Power Control of Isolated Hybrid Power System Including STATCOM and PMG", *Ph.D. Thesis, Centre for Energy Studies, Indian Institute of Technology Delhi, New Delhi (India)*, 2011.

Nomenclature

P_W, P_B, P_G and P_L	Active power output of wind, biogas, grid and load demand respectively.
Q_W, Q_B, Q_G and Q_L	Reactive power output of wind, biogas, grid and load demand respectively.
$\Delta P, \Delta Q$	Change in corresponding active and reactive powers.
$V \angle -\theta, E_G \angle 0^\circ$ and f^0	System bus voltage, Grid source voltage and nominal frequency
$V_{inW}, \angle \delta_{inW}$ and X_T	Inverter input voltage and coupling transformer reactance.
PI1-PI4	Proportional integral controller gains of controllers.
T_{B1} to T_{B7}	Time constants of electronic speed governor, actuator and engine/generator.
$T_{AB}, T_{EB}, T_{FB}, T'_{d0}, T_B$	Various time constants of biogas generator (SG) field and AVR system.
P_{fB}	Power factor of the synchronous (biogas) generator
K_G, K_W, K_B	Generation participation factors of grid, WECS and biogas system, respectively.

Appendix-I

The parameters/constants $V_{inW}, \delta_{inW}, K_{W1}, K_{W2}, \dots, K_{W8}$ of eqns. (7) - (10) are given as

$$V_{inW} = \sqrt{\frac{(P_W X_{TW})^2 + (Q_W X_{TW} + V^2)^2}{V^2}} \quad A.1$$

$$\delta_{inW} + \theta = \sin^{-1}\left(\frac{P_W X_{TW}}{V_{inW} V}\right) \quad A.2$$

$$K_{W1} = K_{W2} = \frac{V_{inW} V \cos(\delta_{inW} + \theta)}{X_{TW}} \quad A.3$$

$$K_{W3} = \frac{V \sin(\delta_{inW} + \theta)}{X_{TW}} \quad A.4$$

$$K_{W4} = \frac{V_{inW} \sin(\delta_{inW} + \theta)}{X_{TW}} \quad A.5$$

$$K_{W5} = K_{W6} = -\frac{V_{inW} V \sin(\delta_{inW} + \theta)}{X_{TW}} \quad A.6$$

$$K_{W7} = \frac{V \cos(\delta_{inW} + \theta)}{X_{TW}} \quad A.7$$

$$\text{And, } K_{W8} = \frac{V_{inW} \cos(\delta_{inW} + \theta) - 2V}{X_{TW}} \quad A.8$$

The parameters/constants of equations (14) and (16) are given as

$$T_{GB} = \frac{X'_{dB} T'_{doB}}{X_{dB}} \quad A.9$$

$$K_{1B} = \frac{X'_{dB}}{X_{dB}} \quad A.10$$

$$K_{2B} = \frac{(X_{dB} - X'_{dB}) \cos(\delta + \theta)}{X_{dB}} \quad A.11$$

$$K_{3B} = \frac{V \cos(\delta + \theta)}{X'_{dB}} \quad A.12$$

$$K_{4B} = \frac{E'_{qB} \cos(\delta + \theta) - 2V}{X'_{dB}} \quad A.13$$

$$\text{And, } K_{RB} = \frac{\sqrt{(1 - P_{fb}^2)}}{P_{fb}} \quad A.14$$

The constants K_{1G} , K_{2G} , K_{3G} , K_{4G} of equations (17) and (18) are given as

$$K_{1G} = \frac{E_G V \cos \theta}{X_G} \quad A.15$$

$$K_{2G} = \frac{E_G \sin \theta}{X_G} \quad A.16$$

$$K_{3G} = \frac{E_G V \sin \theta}{X_G} \quad A.17$$

$$K_{4G} = \frac{E_G \cos \theta - 2V}{X_G} \quad A.18$$

Appendix-II

The system consists of a cluster of 04 medium size villages in India to be supplied by the rural electric supply system under consideration. The data of the system is given below:
 Number of houses (average) in a village = 400 with total number of houses to be supplied = 1600
 The electric contract demand of a house as per Indian conditions = 1 kW (approximately)
 Total contract demand (domestic), A = 1600 kW

Number of irrigation pumps per village = 10 of size/rating of each pump = 5 kW

Total contract demand for irrigation, B = 200 kW

Total contract demand for other amenities in the villages such as street lighting, shops, small hospital/dispensary, school, community hall, religious places (Gurudwara, Temple, Mosque, Church etc.), C = 20 kW

Total contract demand of the four villages = A+B+C = 1600+200+20 = 1820 kW

The maximum diversified demand = 1820*0.55 = 1000 kW

The nominal load of the system, $P_L = 1000$ kW, and it depends on the load curve of the day.

Table A.1: Generation and rated capacity of the system

Sources	Generation $P_G^0 = P_L$ (kW)	Rated capacity (kW)
Grid	300	350
Biogas	500	750
Wind	200	400
Total	1000	1500

Base power = 1500 kW and load $P_L = 1000$ kW

Nominal frequency of the system $f^0 = 50$ Hz.

Gain constant of the system, $K_P = 75$ Hz /pu kW

Time constant of the system, $T_P = 15$ sec.

Nominal voltage of the system $V = 1.0$ pu

Reactive power gain constants of the system,

$K_V = 1.5$ pu kV/pu kVAR

Time constant of the system, $T_V = 0.00212$

The active power participation factors of the sources in system are

$K_G = 300/1500 = 0.2$

$K_B = 500/1500 = 0.33335$

$K_W = 200/1500 = 0.13335$

$K_G + K_B + K_W = 1000/1500 = 0.6667$

Grid

$P_G = 0.2$ pu kW

$Q_G = 0.09686$ pu kVAR

$K_{1G} = -2.8746$

$K_{2G} = 0.2$

$K_{3G} = 0.2$

$K_{4G} = -2.6809$

Wind

$P_W = 0.13335$ pu kW

$Q_W = 0.24169$ pu kVAR

$T_W = 1.0$ sec

$K_{W1} = K_{W2} = 3.0$

$K_{W3} = 0.1225$

$K_{W4} = 0.13335$

$K_{W5} = K_{W6} = -0.13335$

$K_{W7} = 2.75768$

$K_{W8} = -2.5188$

Biogas

$P_B = 0.33335$

$Q_B = 0.16145$

$X_d = 1.0$ pu

$X_d' = 0.15$ pu

$T_{d0}' = 5.0$ sec

$T_B = 0.75$ sec

$K_{1B} = 0.15$

$K_{2B} = 0.84326$

$K_{3B} = 2.45$

$K_{4B} = -2.308$

$T_{B1} = 0.01$ sec

$T_{B2} = 0.02$ sec

$T_{B3} = 0.15$ sec

$T_{B4} = 0.2$ sec

$T_{B5} = 0.014$ sec

$T_{B6} = 0.04$ sec

$T_{B7} = 0.036$

$K_{AB} = 200$

$T_{AB} = 0.05$ sec

$K_{EB} = 1$

$T_{EB} = 2.0$

$K_{FB} = 0.5$

$T_{FB} = 1.0$ sec

Reactive power participation factor: $K_{RB} = 0.48432$